

## ARTICLES

## Photophysics of 1,8-Bis(dimethylamino)naphthalene in Solution: Internal Charge Transfer with a Twist

Anna Szemik-Hojniak,<sup>\*,†</sup> Grzegorz Balkowski,<sup>‡</sup> George W. H. Wurpel,<sup>‡</sup> Jurek Herbich,<sup>§</sup> Joan H. van der Waals,<sup>||</sup> and Wybren J. Buma<sup>\*,‡,⊥</sup>

Faculty of Chemistry, Wrocław University, 14 Joliot-Curie Str., 50-383 Wrocław, Poland, Institute of Molecular Chemistry, University of Amsterdam, Nieuwe Achtergracht 166, 1018 WV Amsterdam, The Netherlands, Institute of Physical Chemistry, Polish Academy of Science, Kasprzaka 44/52, 01-224, Warsaw, Poland, and Huygens Laboratory, Leiden University, Niels Bohrweg 2, P.O. Box 9504, 2300 RA Leiden, The Netherlands

Received: May 13, 2004; In Final Form: August 27, 2004

The photophysical properties of the excited states of 1,8-(bisdimethylamino)naphthalene have been investigated by a combination of experimental spectroscopic methods and quantum chemical calculations. The experiments show that vertical excitation occurs to an  $^1L_a$ -type state from which internal conversion occurs to a state with dominant internal charge-transfer character. This character gives rise to weak emissive properties, a strong solvent dependence of the emission, and transient absorption spectra that carry the signature of the steady-state absorption spectra of the naphthalene radical anion. The quantum chemical calculations support the interpretation of the experimental studies, and enable us to put their results into a broader perspective. They explain the order of the lower excited states of 1,8-(bisdimethylamino)naphthalene and related compounds as well as the role of intramolecular relaxation upon excitation, thereby elucidating the large Stokes shift already observed in nonpolar solvents.

## I. Introduction

The molecule 1,8-bis(dimethylamino)naphthalene (Figure 1), henceforth called DMAN (Figure 1), is the prima donna among the class of “proton sponges”, bidentate nitrogen bases that combine a strong basicity with a low nucleophilic character.<sup>1,2</sup> The title compound, for example, has a  $pK_a$  of 12.1<sup>3</sup> and a gas-phase proton affinity of 1030 kJ/mol.<sup>4</sup> The properties of proton sponges and their monoprotonated cations have been reviewed in a number of publications.<sup>1,2,5</sup> Until recently, the application of the proton sponges has mainly been limited to their use as auxiliary bases in various organic syntheses.<sup>6</sup> More novel developments include gene therapy<sup>7,8</sup> and their use as model compounds helpful for understanding the mechanisms of enzyme-catalyzed reactions.<sup>9</sup>

Steric strain in competition with resonance and repulsive interactions between the nitrogen lone pairs determine the geometrical structure of DMAN. In the pioneering X-ray study of DMAN by Einspahr et al.<sup>10</sup> it was found that in the solid state the molecule is strained with a nonplanar naphthalene skeleton. One of the reasons why proton sponges have attracted attention is their tendency to form very stable ionic complexes containing asymmetric intramolecular  $[N-H\cdots N]^+$  hydrogen

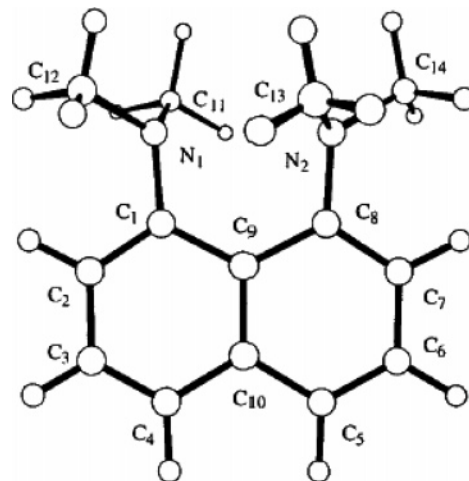


**Figure 1.** Structure and employed atom numbering of the electronic ground state of 1,8-bis(dimethylamino)naphthalene in its lowest energy conformation of  $C_2$  symmetry.

bonds. Upon protonation, substantial changes occur in the geometry of the molecule, causing the molecule to become more planar.<sup>11,12</sup> While it has often been suggested that the relief of electron repulsion is a major driving force for protonation, recent calculations claim that hydrogen bonding is the main contributing factor for the enhanced proton sponge basicity.<sup>13</sup>

The competition between steric and electronic interactions is borne out by the high-resolution spectroscopic studies that we performed some time ago on DMAN seeded in supersonic

\* To whom correspondence should be addressed.

<sup>†</sup> Wrocław University.

<sup>‡</sup> University of Amsterdam.

<sup>§</sup> Polish Academy of Science.

<sup>||</sup> Leiden University.

<sup>⊥</sup> E-mail: wybren@science.uva.nl. Telephone: (31)-20-525 6973/6421. Fax: (31)-20-525 6456/6422.

expansions.<sup>14</sup> In these studies, it was found that the molecule can adopt two conformations in the ground state with strikingly different spectroscopic properties. Ab initio calculations at the HF/6-31G\* level supported this conclusion and revealed that the major difference between the two conformations occurs in the relative positions of the methyl groups in the two dimethylamino groups. The excited-state manifold was investigated in subsequent semiempirical calculations,<sup>15</sup> from which it was concluded that the properties of the lower excited states are rather susceptible to the molecular geometry as exemplified by the reversal of the lower two excited states for the two conformers.

In the present paper we will be concerned with the photophysical properties of DMAN in solution. The ab initio and semiempirical calculations show that some of the orbitals involved in the description of the lower-lying excited states are to a large extent localized on either the dimethylamino groups or the naphthalene skeleton and thus give rise to electronically excited states with charge-transfer character. In solution such polar states are stabilized by solvent-solute interactions and they might thus influence, and possibly even determine, the photophysical behavior of the molecule under such conditions. The excited states of the (substituted) 1-aminonaphthalenes, in many respects analogues of DMAN, serve in this context as an illuminating example. For these molecules inversion of the naphthalene  $S_1(^1L_b)$  and  $S_2(^1L_a)$  states occurs.<sup>16-18</sup> The fluorescent state of these molecules in solution is therefore of  $^1L_a$  parentage and obtains a partial charge-transfer character due to the presence of the amino group. The difference between the  $^1L_a$  and  $^1L_b$  states with respect to this partial charge transfer has been used as an argument to explain the polarity and temperature dependence of the nonradiative decay processes.<sup>19-22</sup>

Already for quite some time it appeared that intramolecular charge transfer (ICT) is indeed a dominating factor in the spectroscopy of DMAN in solution. For the protonated proton sponge a very weak, strongly redshifted emission has been observed and explained in terms of an overlap forbidden transition from a strongly lowered and highly polar charge transfer state which involves two approximately orthogonal orbitals.<sup>23</sup> The situation is far less clear-cut for the neutral molecule. In certain solvents, it seemed that one is dealing with a mixture of two species,<sup>23</sup> but even then it is hard to understand what the origin is of the large Stokes shift observed for one of these species. Since the Stokes shift is sensitive to the charge reorganization on excitation and the interaction with the solvent, one might take this observation as evidence for considerable charge transfer in the excited state.

Another explanation involves geometry relaxation in the excited state. Excitation of the  $^1L_a$  state of the previously mentioned (substituted) 1-aminonaphthalenes is accompanied by significant geometry relaxation, primarily a reorientation of the dimethylamino group.<sup>17,18</sup> This geometry relaxation is determined essentially by the combination of two opposing effects: (i) the resonance interaction between the dimethylamino groups and the aromatic ring and (ii) steric hindrance between the substituents at the *peri* positions. The same interactions are present in DMAN with one important difference, namely the additional repulsive interactions between the nitrogen lone pairs. These observations made us suspect that the excited states of DMAN might equally well be subject to major geometry changes, certainly if they would involve orbitals with contributions from the nitrogen lone pairs.

Here we present the results of experimental studies on the excited states of DMAN in solution with a variety of techniques.

On the basis of the solvent dependence of steady-state absorption and emission spectra, it will be shown that the emissive species in these experiments is an excited state with an increased dipole moment with respect to the ground state. From the radiative decay rate of DMAN, it is concluded that the emissive transition from this state is highly forbidden, an observation which can be understood on the basis of transient absorption experiments. The latter experiments show that (i) a naphthalene radical anion like species is formed upon excitation and (ii) intersystem crossing to the triplet manifold is a significant decay pathway. The conclusions drawn from the experimental studies are subsequently put into the perspective of quantum chemical calculations performed to elucidate the order and specific character of the excited states accessed in the experiments and the role of geometry relaxation upon excitation. The calculations confirm the experimental conclusions and indicate how the molecular geometry responds to various electronic excitations. For the emissive ICT state observed in our experiments they explain the observed Stokes shift in terms of an increased twisting of the dimethylamino groups. For the  $^1L_a$ -like state, on the other hand, an untwisting motion is predicted.

## II. Experimental Section

DMAN was purchased from Aldrich. Experiments were performed on samples as received but also on samples sublimed under vacuum prior to use. In all cases, the same results were obtained.

**Optical Absorption Spectroscopy.** Electronic absorption spectra were recorded on a Hewlett-Packard 8453 diode array spectrophotometer or on a Cary 3 (Varian). Molar absorption coefficients were determined using concentrations of  $10^{-4}$ – $10^{-5}$  M.

**Steady-State Fluorescence Spectroscopy.** Fluorescence spectra were recorded on a Spex Fluorolog 3 emission spectrometer using a spectral bandwidth of  $\leq 2$  nm for both excitation and emission. Fluorescence was detected using a Peltier-cooled R636-10 (Hamamatsu) photomultiplier tube. Emission spectra were corrected for the wavelength-dependent response of the detection system. Fluorescence quantum yields were determined relative to a reference solution of quinine bisulfate in 1 N sulfuric acid ( $\Phi_f = 0.546$ )<sup>24</sup> and corrected for the refractive index of the solvent. The samples were made with an absorbance of ca. 0.1 (1 cm path length) at the excitation wavelength and degassed by purging with argon for 10–15 min. Commercially available spectrograde solvents were used (Merck, Uvasol) and stored over molecular sieves. When the purity of the solvent proved to be insufficient, it was purified by standard procedures.<sup>25</sup>

**Time-Resolved Fluorescence Spectroscopy.** Fluorescence decay curves were measured using a picosecond time-correlated single photon counting setup described in detail before.<sup>26</sup> Excitation was provided by a mode-locked argon ion laser (Coherent 486 AS Mode Locker and Coherent Innova 200 laser) which pumped synchronously a dye laser (Coherent model 700) operating on DCM. The dye laser, frequency-doubled with a BBO crystal, yielded 310–320 nm pulses. A Hamamatsu microchannel plate photomultiplier (R3809) was used as detector. The response function of the instrument has a fwhm of  $\approx 17$  ps.

**Transient Absorption Spectroscopy.** For the measurement of nanosecond transient absorption spectra, the third harmonic of a Coherent Infinity Nd:YAG laser (355 nm, 10 Hz) was employed as excitation source. This laser system delivers 2 ns pulses, the output of which was adjusted to a pulse energy of

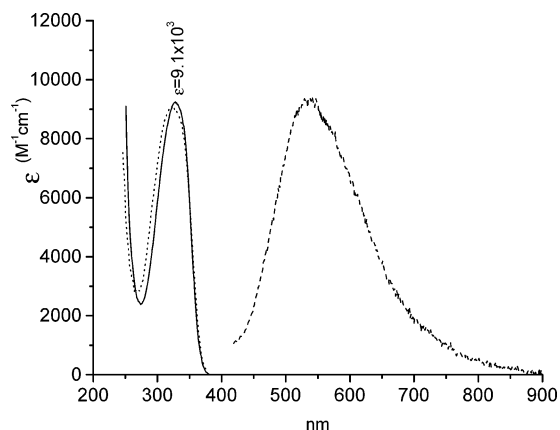


**Figure 2.** Absorption (—), dispersed emission (---), and fluorescence detected excitation (···) spectra of DMAN in *n*-hexane. The dispersed emission spectrum has been obtained for excitation at 330 nm; the fluorescence detected excitation spectrum by monitoring the emission at 540 nm.

approximately 2.5 mJ. A pulsed low-pressure Xe flashlamp (EG&G, FX504) provided the probe light in a perpendicular geometry. The probe light was collected on a Princeton Instruments time-gated (5 ns) intensified CCD camera (Princeton Instruments ICCD-576-G/RB-EM) after passing through a spectrograph (Acton SpectraPro-150). The detector was gated at 5 ns. Typically 50 spectra were averaged to obtain a satisfactory signal-to-noise ratio. Typical absorbance of the samples at the excitation wavelength was 1–2 over 1 cm. The time-dependent behavior of excited triplet species was monitored in a separate experiment with a 450 W Xe arc (Müller lamp housing LAX1450, power supply SVX1450), an electronic pulser (Vincent Associates SP05), an Oriel monochromator, and a photomultiplier (1P28, S5 photocathode) coupled to a Tektronix TDS684B oscilloscope as the probe system, and the same laser as the excitation source. The transient absorption samples were carefully degassed by at least three freeze–pump–thaw cycles using a T-cell. During acquisition, the cell was stirred to minimize buildup of possible photodegradation products in the excitation volume.

### III. Results and Discussion

**A. Experimental Studies.** In Figure 2, the absorption spectrum of DMAN in *n*-hexane is displayed. In previous studies of DMAN in solution it was tentatively concluded that the molecule exhibits dual fluorescence,<sup>23</sup> although at that time its nature could not be further clarified. Here we find that excitation at the relatively strong absorption band at 330 nm leads to an emission spectrum with only one band at 536 nm (Figure 2). This emission band is rather weak—the fluorescence quantum yield is only 0.0014—but the excellent correspondence between the fluorescence detected excitation spectrum (Figure 2) and the absorption spectrum strongly suggests that the 536 nm band derives from DMAN. The apparent disagreement between the previous results, which indicated a dual fluorescence, and the present results, which do not give evidence for this phenomenon, is puzzling. We have not gone at full length to find an explanation but remark that we have noticed that it is imperative to make sure that water is removed from samples and solvents. If this is not done carefully, one is able to observe an additional emission band around 410 nm. Moreover, experiments in which solutions were illuminated with a mercury lamp filtered with a WG320 filter showed changes in the emission spectrum in the course of time, indicating that also photochemistry may occur.

**TABLE 1: Spectral Properties of DMAN in Various Solvents**

solvent	$\Delta f^a$	$\lambda_{\text{max}}^{\text{abs}}$ (nm)	$\tilde{\nu}_{\text{max}}^{\text{flu}}$ <sup>b</sup> (cm <sup>-1</sup> )
<i>n</i> -hexane	0.092	330	18195
3-methylpentane	0.093	330	18147
di- <i>n</i> -butyl ether	0.194	332	16988
diethyl ether	0.251	332	16671
ethyl acetate	0.292	333	16344
tetrahydrofuran	0.308	335	15803
dichloromethane	0.319	336	15400
acetonitrile	0.393	337	c

<sup>a</sup> Defined by eq 2. <sup>b</sup> Corrected for  $\lambda^2$  factor. <sup>c</sup> Not observed.

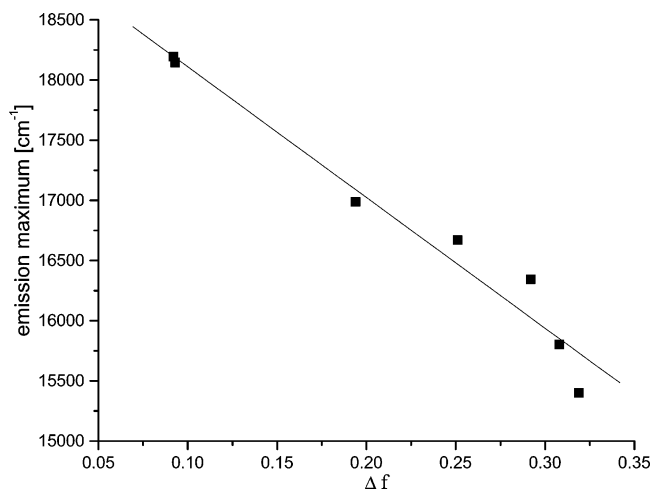


**Figure 3.** Solvent dependence of the emission maximum of DMAN. The line is a fit to eq 1 yielding an intercept of  $18616 \pm 25$  cm<sup>-1</sup> and a slope of  $-6803 \pm 149$  cm<sup>-1</sup>.

A second issue that needs to be dealt with in these solution studies concerns the role of the two conformers observed in our previous gas-phase studies.<sup>14</sup> As will become clear in the discussion below, the present study does not give any indication that a second conformation needs to be invoked to explain the results. In the gas-phase studies the second conformation was only observed at elevated temperature, making it indeed plausible that in the present studies performed at room temperature one species is predominantly present.

Table 1 reports the dependence of the spectral properties of DMAN on the solvent polarity. We find that the absorption maximum hardly changes, whereas the emission maximum is strongly influenced by the solvent polarity. The latter dependence indicates that the dipole moment of the electronic ground state and the state from which emission takes place is significantly different. In the Onsager cavity approach, the solvatochromic shift of the emission band is given by<sup>27,28</sup>

$$\Delta\tilde{\nu}_{\text{fl}} = \tilde{\nu}_{\text{fl}}(\Delta f) - \tilde{\nu}_{\text{fl}}(0) = \frac{-\mu_e(\mu_e - \mu_g)}{2\pi\epsilon_0 hca^3} \Delta f \quad (1)$$

where  $a$  is the Onsager radius of the solute and  $\Delta f$  is defined by the dielectric constant  $\epsilon$  and the refractive index  $n$  of the solvent as

$$\Delta f = \frac{(\epsilon - 1)}{2\epsilon + 1} - \frac{(n^2 - 1)}{4n^2 + 2} \quad (2)$$

The fit of the emission maxima to eq 1 is depicted in Figure 3, and results in values for the fit parameters  $\tilde{\nu}_{\text{fl}}(0)$  and  $\mu_e(\mu_e - \mu_g)/2\pi\epsilon_0 hca^3$  of  $19195 \pm 231$  cm<sup>-1</sup> and  $10860 \pm 967$  cm<sup>-1</sup>, respectively. For the ground state of DMAN a dipole moment

$\mu_g$  of 1.12 D has been reported.<sup>29</sup> To estimate the dipole moment of the excited state, we assume that the Onsager radius  $a$  can be determined using the reported molecular density of 1.12 g/cm<sup>3</sup><sup>10</sup> and Avogadro's number,<sup>30</sup> leading to a value of 4.2 Å. Under the additional, but reasonable, assumption that the dipole moments of the molecule in the ground and excited states are parallel, a value of 9.5 D is calculated for  $\mu_e$ .

In what is to follow, we will conclude that the observed emission represents the radiative decay of an electronic state with a predominant charge-transfer character. Anticipating this result, we may employ the dipole moment  $\mu_e$  of the emissive state to estimate the fraction of charge displaced upon excitation. Assuming that the dimethylamino groups form the electron donor and the naphthalene ring the electron acceptor, and using the structure parameters as determined experimentally,<sup>10</sup> we conclude that about 0.7 electron is transferred upon excitation from the ground state.

For a solution of DMAN in *n*-hexane we find that the emission at 536 nm can be fitted satisfactorily in terms of a single exponential with a decay constant of 2.2 ns. In combination with the observed fluorescence quantum yield of 0.0014, this would imply that the emissive state has a radiative decay rate of  $6.4 \times 10^5$  s<sup>-1</sup>. When absorption and emission occur to and from the same electronically excited state, one can obtain the radiative transition probability from the absorption and emission spectra via the Strickler–Berg relationship.<sup>31</sup> Application of this relationship to DMAN in *n*-hexane leads to incompatible results between observed (on the order of  $10^5$  s<sup>-1</sup>) and calculated (on the order of  $10^7$  s<sup>-1</sup>) radiative decay rates. One therefore has to conclude that the state that is responsible for the absorption band around 330 nm is not the emissive state observed in the fluorescence spectrum.

For 1-aminonaphthalene, 1-(methylamino)naphthalene, and 1-(dimethylamino)naphthalene in *n*-hexane, radiative decay rates of 6.6, 7.4, and  $8.3 \times 10^7$  s<sup>-1</sup><sup>21</sup> have been determined. We recall that in these molecules the emissive state has <sup>1</sup>L<sub>a</sub> character, which accounts for the relatively large decay rates. In the first instance, one might expect the electronic structure of DMAN and these 1-aminonaphthalenes to be similar. The observed reduction of the radiative decay rate in DMAN by almost 2 orders of magnitude, however, stands in stark contrast with this notion, and one has to conclude that the character of the emissive state in DMAN is fundamentally different, i.e., is not of L<sub>a</sub> parentage.

Figure 4 displays transient absorption spectra of DMAN in *n*-hexane up to a delay time of 50 ns. From the time dependence of the transient absorption spectrum, one concludes that it contains two components: the first component decays within the time resolution of the detection system while a second component decays on a much longer time scale. The latter component is explicitly monitored in Figure 5 where the decay of the transient absorption signal at 580 nm is shown for delay times up to 18 μs. The susceptibility of the long-lived component toward molecular oxygen indicates that the signal derives from transient absorption from the T<sub>1</sub> state. It is known that triplet decays in solution are in general rarely truly monoexponential. In line with this experience, we find that the triplet decay can only be fitted with a pseudo monoexponential decay if we restrict the analysis to delay times larger than 5 μs. We thus obtain a decay constant of  $8.0 \pm 0.2$  μs. The observation of transient absorption in the triplet manifold establishes that one of the nonradiative decay pathways in the molecule is intersystem crossing, but at this point it is difficult to say whether

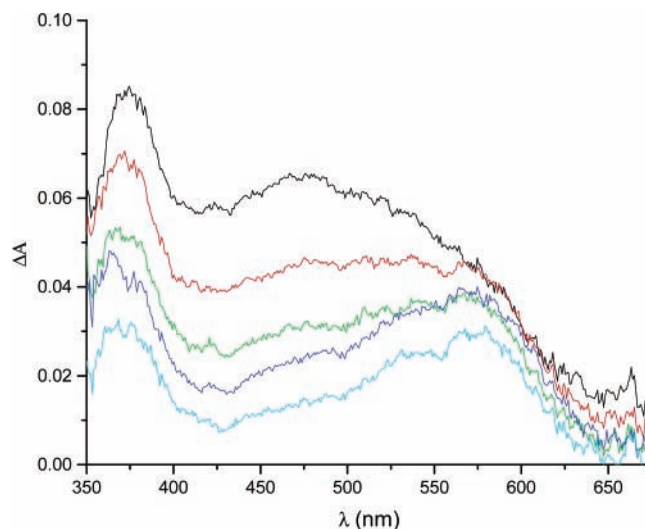


**Figure 4.** Fluorescence corrected transient absorption spectra of a degassed solution of DMAN in *n*-hexane obtained 0 (black), 2 (red), 4 (green), 10 (blue), and 60 (cyan) ns after excitation with a 355 nm laser pulse.

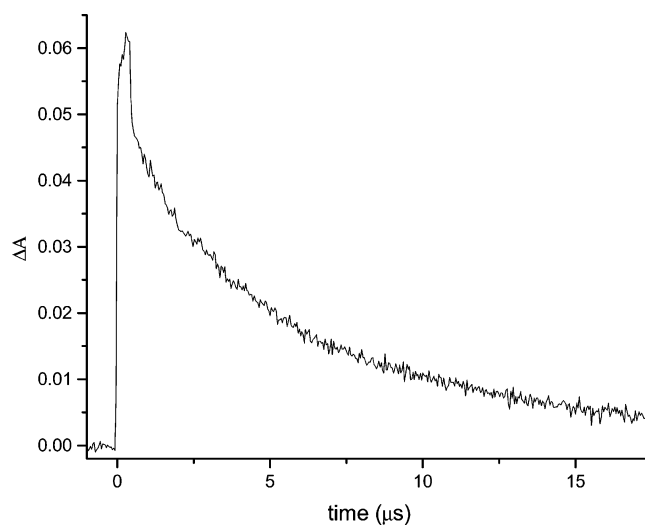


**Figure 5.** Decay of the transient absorption spectrum of a degassed solution of DMNA in *n*-hexane excited at 355 nm and probed at 580 nm.

it is the dominant one since we have not determined absolute triplet quantum yields.

The fast component in the transient absorption spectra of Figure 4 is assigned to absorption from the (relaxed) S<sub>1</sub> state. In Figure 6a we have reconstructed the associated S<sub>n</sub> ← S<sub>1</sub> transient absorption spectrum by subtracting the triplet absorption spectrum (vide infra) from a spectrum taken directly after the laser pulse. It shows a narrow absorption band around ca. 380 nm and a very broad absorption in the 580–400 nm wavelength region that might contain some weak structure. These features differ fundamentally from what one would expect for transient absorption of a substituted naphthalene species: the S<sub>n</sub> ← S<sub>1</sub> spectrum of naphthalene displays a broad peak around ca. 420 nm and a very weak absorption in the 700–450 nm region,<sup>32</sup> a pattern that has been observed in picosecond time-resolved transient absorption spectra of rigidly linked naphthalene-trialkylamine compounds in apolar solvents as well.<sup>33</sup> The singlet transient absorption spectrum compares, on the other hand, favorably with the steady-state absorption spectra of the radical anion of naphthalene and 1,8-diaminonaphthalene.<sup>34,35</sup> For the naphthalene radical anion in MTHF one

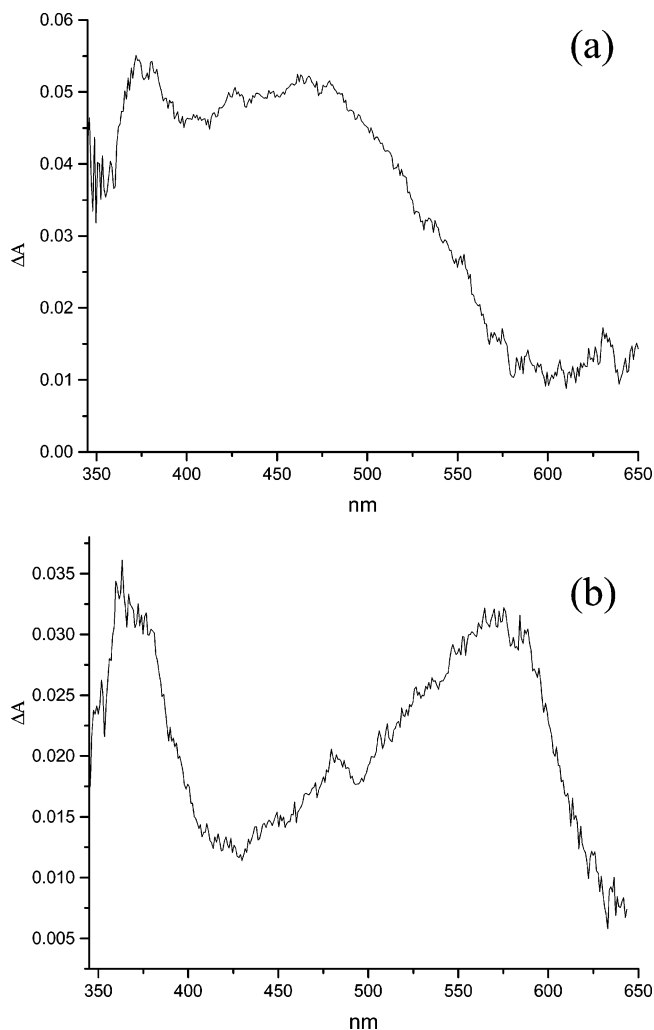


**Figure 6.**  $S_n \leftarrow S_1$  absorption (a) and  $T_n \leftarrow T_1$  absorption (b) of DMAN in *n*-hexane. The triplet absorption spectrum was taken 1  $\mu$ s after the laser pulse, and the singlet absorption was obtained by subtracting the triplet spectrum from a spectrum taken directly after the laser pulse.

observes (i) a band system with peaks at 775 and 840 nm that extends up to 600 nm, (ii) a broad, weakly structured absorption that starts around 550–530 nm and extends up to 400 nm, and a relatively narrow absorption band around ca. 370 nm. All these features are present in the singlet transient absorption spectrum of DMAN. The main difference between the two spectra is the relative intensity of the 370 nm band, which is larger in absorption spectrum of the naphthalene radical anion. At the same time it should be noticed that the relative intensity of this band in Figure 6 is very sensitive to the way in which the singlet spectrum in Figure 6 has been constructed. We therefore conclude that the singlet transient absorption spectrum indicates that a naphthalene radical anion-like species is formed upon excitation of DMAN.

The  $T_n \leftarrow T_1$  transient absorption spectrum, derived from the transient absorption spectrum observed for a delay of 1  $\mu$ s, is given in Figure 6b. This spectrum shows two absorption bands: one relatively narrow band at ca. 370 nm and a broad absorption band that starts at ca. 580 nm. The latter band extends over a large wavelength range and seems to be composed of more than one band, although our present signal-to-noise ratio prevents us from making more definite conclusions. The  $T_n \leftarrow T_1$  transient absorption spectrum of naphthalene<sup>32</sup> and rigidly linked naphthalene-trialkylamine species in apolar solvents<sup>33</sup> exhibits only a band around 420 nm. The additional band around

580 nm in DMAN might therefore indicate that also in the triplet manifold absorption occurs from an excited state with a considerable internal charge-transfer character.

**B. Ab Initio and TD-DFT Calculations.** From the experimental material discussed above we conclude that the state responsible for the highly red-shifted weak emission is a state with major contributions from internal charge transfer (ICT) configurations. This state is not directly accessed in our experiments, but appears to become populated after internal conversion from a state with a relatively large oscillator strength. The electronic structure of DMAN has been investigated in the past by semiempirical calculations, in particular in the context of possible differences between the two conformers that had been observed under isolated conditions.<sup>15</sup> At the time it was thought that the lower two excited singlet states were the analogues of the naphthalene  $L_a$  and  $L_b$  states which in DMAN might become quasi-degenerate—and thus very susceptible to small changes in the molecular geometry—and contain charge transfer character due to the mixed character of the HOMO orbital. This charge transfer character is in line with the present experimental findings, but at the same time, it leaves us with pertinent questions about the precise character of the state which is observed in solution and how to reconcile the relatively small dipole moments calculated for the relevant excited states with the dipole moment here determined experimentally.

To elucidate these issues we have extended the previous calculations to the ab initio level. Theoretical studies on the excited states of and internal charge transfer phenomena in 4-(dimethylamino)benzotrile (DMABN) have demonstrated that the results depend critically on the methodology employed<sup>36–38</sup> and that one needs to be cautious in relating their results to experimental data. Levels like CASSCF, CASPT2, and CC2 would be recommended, but are prohibited by the size of DMAN. We were therefore restricted—bearing the previously mentioned pitfalls in mind—to perform calculations at the CI-Singles (CIS) and time dependent density functional theory (TD-DFT) levels. These calculations have been carried out with the GAUSSIAN 98 suite of programs.<sup>39</sup> In previous calculations at the HF/6-31G\* level, we have established that DMAN can adopt two conformations in the ground state, the one of lowest energy having an approximate  $C_2$  symmetry.<sup>14</sup> This conformation is the starting point for the present considerations, although we re-optimized its geometrical parameters at the B3LYP/6-31G\* level<sup>40–42</sup> and imposed  $C_2$  symmetry.<sup>43</sup> Since further on we will be interested in the geometry changes upon electronic excitation, we report the relevant geometrical parameters of this  $C_2$  geometry in Table 2. As expected, the differences with the previously reported  $C_1$  geometry are minor.

When a CIS calculation is performed at the  $C_2$  ground state geometry, we find that only the  $S_1$ ,  $S_2$ , and  $S_3$  excited states are of present interest; the other states are calculated to lie at least 2 eV higher than  $S_1$ . The results obtained for these three states are reported in Table 3. Apart from the transition energies, which are systematically overestimated, we find that the CIS results are qualitatively in agreement with what was calculated at the semiempirical level: the  $S_1$  and  $S_2$  states have similar vertical excitation energies and they carry the signatures of the  ${}^1L_a$  and  ${}^1L_b$  states of naphthalene (respectively of symmetry A and B in the group  $C_2$ ). The three relevant molecular orbitals, 56 (HOMO-2), 57 (HOMO-1), and 58 (HOMO), from which excitation takes place, have significant contributions of the lone pair orbitals on the nitrogen atoms of the dimethylamino groups, while the orbitals to which the electron is excited, 59 (LUMO)

**TABLE 2: Geometrical Parameters (Å and deg) of the  $1^1A$  ( $S_0$ ) Neutral Ground State, the  $1^2B_2$  ( $T^{-1}$ ) and  $1^2A$  ( $\pi_5^{-1}$ ) Radical Cationic States, and the  $1^3B_1$  ( $l\pi_6^*$ ) and  $1^3A$  ( $\pi_5 \pi_6^*$ ) Triplet States Obtained at the (U)B3LYP/6-31G\* Level**

	$1^1A$ ( $C_2$ )	$1^2B_2$ ( $C_{2v}$ )	$1^2A$ ( $C_2$ )	$1^3B_1$ ( $C_{2v}$ )	$1^3A$ ( $C_2$ )
C <sub>1</sub> –C <sub>2</sub>	1.390	1.380	1.425	1.418	1.454
C <sub>2</sub> –C <sub>3</sub>	1.409	1.415	1.388	1.387	1.364
C <sub>3</sub> –C <sub>4</sub>	1.371	1.376	1.391	1.404	1.424
C <sub>4</sub> –C <sub>10</sub>	1.421	1.420	1.414	1.419	1.412
C <sub>9</sub> –C <sub>10</sub>	1.442	1.430	1.442	1.445	1.455
C <sub>1</sub> –C <sub>9</sub>	1.452	1.421	1.446	1.417	1.436
C <sub>1</sub> –N <sub>1</sub>	1.418	1.442	1.369	1.440	1.405
N <sub>1</sub> –C <sub>11</sub>	1.462	1.463	1.463	1.459	1.458
N <sub>1</sub> –C <sub>12</sub>	1.452	1.463	1.468	1.459	1.450
C <sub>9</sub> –C <sub>1</sub> –C <sub>2</sub>	119.2	120.8	118.2	121.8	119.7
C <sub>1</sub> –C <sub>2</sub> –C <sub>3</sub>	122.2	120.1	121.4	119.0	121.3
C <sub>2</sub> –C <sub>3</sub> –C <sub>4</sub>	119.8	120.5	120.1	120.8	119.5
C <sub>3</sub> –C <sub>4</sub> –C <sub>10</sub>	120.5	120.9	120.4	121.6	121.3
C <sub>4</sub> –C <sub>10</sub> –C <sub>9</sub>	120.6	118.8	120.2	118.2	120.1
C <sub>10</sub> –C <sub>9</sub> –C <sub>1</sub>	117.0	119.0	117.0	118.6	116.8
C <sub>1</sub> –C <sub>9</sub> –C <sub>8</sub>	126.0	122.0	126.0	122.7	126.3
C <sub>4</sub> –C <sub>10</sub> –C <sub>5</sub>	118.9	122.4	119.5	123.6	119.8
C <sub>9</sub> –C <sub>1</sub> –N <sub>1</sub>	120.9	118.0	122.7	117.8	121.7
C <sub>1</sub> –N <sub>1</sub> –C <sub>11</sub>	115.6	116.3	121.8	116.8	119.0
C <sub>1</sub> –N <sub>1</sub> –C <sub>12</sub>	117.7	116.3	121.2	116.8	120.0
C <sub>1</sub> –C <sub>2</sub> –C <sub>3</sub> –C <sub>4</sub>	3.2	0.0	1.8	0.0	0.2
C <sub>3</sub> –C <sub>4</sub> –C <sub>10</sub> –C <sub>9</sub>	–1.7	0.0	–1.3	0.0	–0.5
C <sub>4</sub> –C <sub>10</sub> –C <sub>9</sub> –C <sub>1</sub>	8.8	0.0	14.5	0.0	9.7
C <sub>10</sub> –C <sub>9</sub> –C <sub>1</sub> –C <sub>2</sub>	–9.9	0.0	–19.4	0.0	–14.0
C <sub>10</sub> –C <sub>9</sub> –C <sub>1</sub> –N <sub>1</sub>	169.3	180.0	155.9	180.0	163.0
C <sub>9</sub> –C <sub>1</sub> –N <sub>1</sub> –C <sub>11</sub>	–64.3	–109.9	–29.1	–109.8	–51.1
C <sub>9</sub> –C <sub>1</sub> –N <sub>1</sub> –C <sub>12</sub>	160.5	109.9	169.3	109.8	162.3
$\Theta^a$	42.4	–90.0	22.3	–90.0	35.9
$\Sigma N^b$	344.8	347.5	357.7	347.8	351.9

<sup>a</sup> Defined by the average of the two dihedral angles C<sub>2</sub>C<sub>1</sub>N<sub>1</sub>C<sub>12</sub> and C<sub>9</sub>C<sub>1</sub>N<sub>1</sub>C<sub>11</sub>. <sup>b</sup> Sum of valence angles around nitrogen atom.

and 60 (LUMO+1), are essentially the  $\pi_6^*$  and  $\pi_7^*$  orbitals of naphthalene.

Comparison of the CIS results with the experimental material gives rise to a number of problems. First, the experiments have shown that the radiative decay rate is small, which is at odds with a hypothesis that the emission would stem from an  $1^1L_a$ -type of state. Second, the solvent dependence of the emission has demonstrated that the dipole moment of the emissive state is significantly larger than the dipole moment of the ground state. This seems to rule out the  $S_1$  and  $S_2$  states since their calculated dipole moment are almost equal to that of the ground state. One might argue that the calculations have been performed at the equilibrium geometry of the ground state while emission occurs from the equilibrium geometry of the emissive state, but the naphthalene-like  $\pi\pi^*$  character of  $S_1$  and  $S_2$  makes large changes in their dipole moment unlikely. Third, the small oscillator strength and relatively large dipole moment of  $S_3$  would make this state a more likely candidate for the emissive state, but its calculated vertical excitation energy implies that very large internal and solvent reorganization energies would be needed to account for the experimentally observed Stokes shift of  $\sim 12000$  cm<sup>-1</sup> in nonpolar solvents. Problems similar to those we encounter here for DMAN have been reported for CIS calculations on DMABN.<sup>36,37</sup> We therefore conclude that this level of calculation does not suffice for the present study.

Table 3 shows that the situation changes drastically when calculations are performed with the TD-DFT approach. The lowest vertically excited singlet state is now in first order described by the (HOMO-1)  $\rightarrow$  LUMO excitation, which, following Kasha and Rawls<sup>44</sup> will henceforth be designated as the  $l\pi_6^*$  configuration. This state has become nearly degenerate

with the excited state dominated by the  $\pi_5 \pi_6^*$  configuration, i.e., the analogue of the  $1^1L_a$  state, while the  $1^1L_b$  state has become  $S_3$ . The vertical excitation energy calculated for the two lower excited states is in excellent agreement with the maximum of the first absorption band in apolar solvents. Although the absolute vertical excitation energies of the two  $\pi\pi^*$  states have changed by more than 1 eV, we notice that the energy gap between them has remained more or less the same. It is the  $l\pi_6^*$  state that is poorly described at the CIS level, which makes it clear that one requires the incorporation of the dynamic electron correlation intrinsic in the TD-DFT approach.

Figure 7 shows orbital shapes of the relevant molecular orbitals forming the basis for the TD-DFT description of the various excited states. What is evident from these orbitals is that the lowest excited singlet state can in first approximation indeed be described as a state in which an almost full internal charge transfer has occurred: the  $l$  and  $\pi_6^*$  orbitals are highly localized on the two dimethylamino groups and the naphthalene ring, respectively. The contour plots also show that the  $1^1L_a$  state contains charge-transfer character as well because of the participation of the lone-pair orbitals in the HOMO. Comparison with contour plots of the HF/6-31G\* orbitals (not shown) employed for the CIS description demonstrates that the dimethylamino lone-pair electrons are much more delocalized in the HF approach; in particular a significant contribution is found in the  $\pi_4$  orbital.

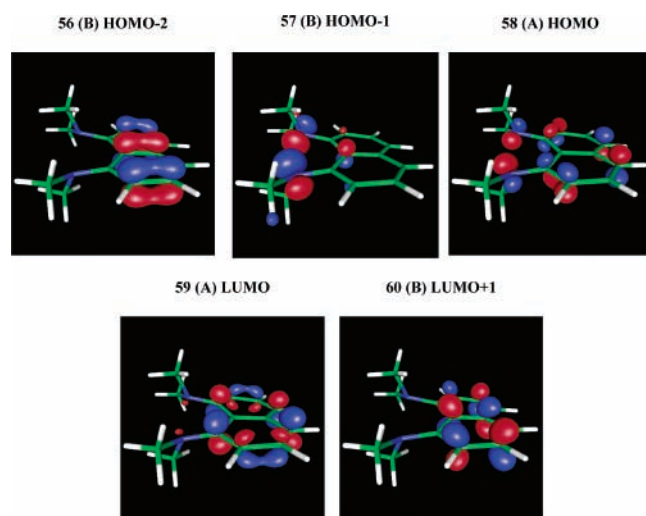
It is interesting to consider the present results on DMAN in the light of what is known for 1-(dimethylamino)naphthalene. Above we have concluded that the emissive states in the two molecules have fundamentally different properties: the lowest excited singlet state of 1-(dimethylamino)naphthalene has a dominant  $L_a$  character,<sup>16,18,20</sup> which is responsible for the relatively large radiative rates, while in DMAN emission occurs from an internal charge transfer state with a small electronic transition moment to the ground state. How should we understand the differences between the excited states manifolds of the two molecules? To answer this question, we have performed TD-DFT calculations on the excited states of 1-(dimethylamino)naphthalene<sup>45</sup> at the B3LYP/6-31G\* optimized geometry of the ground state.<sup>46</sup> Before comparing the excited states of the two molecules, it is instructive to compare their ground-state structures. As expected, the major difference between the two molecules occurs in the orientation of the dimethylamino group relative to the naphthalene plane. In the ground state of DMAN, the twist angle  $\Theta$ —defined by the average of the two dihedral angles C<sub>2</sub>C<sub>1</sub>N<sub>1</sub>C<sub>12</sub> and C<sub>9</sub>C<sub>1</sub>N<sub>1</sub>C<sub>11</sub> (see Figure 1)—is 42.4°; in 1-(dimethylamino)naphthalene it is 49.7°. Another way that the steric strain between the dimethylamino groups and the associated lone pair repulsions in DMAN might be minimized is by changing the hybridization of one or both of the nitrogen atoms, as occurs, for example, in the other conformer of DMAN observed in the gas phase.<sup>14</sup> From the sum of the valence angles of the amino nitrogen atom (344.8 and 342.4° in DMAN and 1-(dimethylamino)naphthalene, respectively), we conclude, however, that this does not occur; i.e., the nitrogen atoms are similarly hybridized in both molecules.

Table 3 reports the results of the TD-DFT calculations on 1-(dimethylamino)naphthalene. Orbital contour plots reveal that the  $\pi_4$ ,  $\pi_6^*$ , and  $\pi_7^*$  orbitals of 1-(dimethylamino)naphthalene can be compared directly with their counterparts in DMAN. The  $l$  and  $\pi_5$  orbitals, on the other hand, are slightly more delocalized over the naphthalene ring and dimethylamino group, respectively, than the analogous orbitals in DMAN. Compared to DMAN we find that the  $1^1L_a$  and  $1^1L_b$  states in 1-(dimethyl-

**TABLE 3: Description and Properties of the Lower-lying Electronic Excited Singlet States of DMAN and 1-(Dimethylamino)naphthalene at Their B3LYP/6-31G\* Optimized  $S_0$  Geometries, Where for Clarity the Dominant Contribution to the Wave Function of the Various Excited States is Indicated in Bold Italics**

excited state	DMAN CI-Singles				DMAN TD-DFT			1-(dimethylamino)naphthalene TD-DFT		
	wave function composition <sup>a</sup>	$\Delta E$ (eV)	oscillator strength <sup>f</sup>	$\mu^b$ (D)	wave function composition <sup>c</sup>	$\Delta E$ (eV)	oscillator strength <sup>f</sup>	wave function composition <sup>d</sup>	$\Delta E$ (eV)	oscillator strength <sup>f</sup>
$S_1$	-0.17 (56 $\rightarrow$ 60) -0.22 (57 $\rightarrow$ 60) <b>+0.62 (58 <math>\rightarrow</math> 59)</b> (A)	4.95	0.211	1.4	<b>0.68 (57 <math>\rightarrow</math> 59)</b> (B)	3.84	0.014	0.16 (45 $\rightarrow$ 47) <b>+0.64 (46 <math>\rightarrow</math> 47)</b>	3.93	0.100
$S_2$	0.28 (56 $\rightarrow$ 59) +0.28 (57 $\rightarrow$ 59) <b>+0.57 (58 <math>\rightarrow</math> 60)</b> (B)	5.15	0.050	1.3	-0.12 (56 $\rightarrow$ 60) <b>+0.65 (58 <math>\rightarrow</math> 59)</b> (A)	3.85	0.143	0.39 (44 $\rightarrow$ 47) -0.13 (45 $\rightarrow$ 47) <b>+0.58 (46 <math>\rightarrow</math> 48)</b>	4.34	0.010
$S_3$	-0.34 (56 $\rightarrow$ 59) <b>+0.53 (57 <math>\rightarrow</math> 59)</b> -0.25 (58 $\rightarrow$ 61) (B)	6.05	0.086	4.3	0.34 (56 $\rightarrow$ 59) <b>+0.62 (58 <math>\rightarrow</math> 60)</b> (B)	4.12	0.053	0.12 (44 $\rightarrow$ 47) 0.15 (44 $\rightarrow$ 48) <b>+0.64 (45 <math>\rightarrow</math> 47)</b> -0.10 (46 $\rightarrow$ 47)	4.80	0.011

<sup>a</sup> The highest occupied molecular orbital (HOMO) in the ground-state  $S_0$  is MO 58; this orbital contains a significant contribution from the  $\pi_5$  orbital of naphthalene. Orbitals 56 and 57 are mixtures of the  $\pi_4$  orbital of naphthalene and the antisymmetric combination of the lone pair orbitals on the amino groups. Orbitals 59 and 60 are the quasi-pure  $\pi_6^*$  and  $\pi_6^*$  orbitals of naphthalene. Symmetry of state in  $C_2$  is given in parentheses.<sup>b</sup> The dipole moment calculated for the ground-state  $S_0$  is 1.4 D. <sup>c</sup> Orbital contours are shown in Figure 7. Symmetry of state in  $C_2$  is given in parentheses. <sup>d</sup> The highest occupied molecular orbital (HOMO) in the ground-state  $S_0$  is MO 46. Orbitals are approximately be described as follows: 44 =  $\pi_4$ ; 45 = 1; 46 =  $\pi_5$ ; 47 =  $\pi_6^*$ ; 48 =  $\pi_7^*$ .

**Figure 7.** Orbital shapes of B3LYP/6-31G\* orbitals of DMAN relevant for the description of the lower excited states.

amino)naphthalene are at only slightly higher excitation energies (0.08 and 0.22 eV, respectively), but the excitation energy of the  $1\pi_6^*$  state is raised by almost 1 eV. These changes parallel quite nicely the differences in orbital energies: the  $\pi$  orbitals are hardly influenced but the 1 orbital is lowered by more than 1.0 eV. We therefore conclude that the vertical excitation energy of the  $1\pi_6^*$  ICT state is so significantly lowered in DMAN compared to 1-(dimethylamino)naphthalene because the steric strain and lone pair repulsion induced by the second dimethylamino group raises the energy of the 1 orbital.

A final issue that needs to be elucidated is the experimentally observed Stokes shift, which is associated with solvent reorganization and relaxation of the geometry of the molecule on excitation. The observation that for DMAN a Stokes shift of about 1.4 eV is already observed in nonpolar solvents—where solvent reorganization effects are only minor—implies a dominant contribution of the internal reorganization energy. Considering the nature of the ICT state, a significant difference between the geometry of the molecule in the vertically excited

and the adiabatic ICT state can a priori indeed be expected. After all, excitation of an electron from the 1 orbital into the naphthalene ring reduces the charge density in the lone pair orbital of each of the nitrogen atoms and thereby the repulsion between their charge densities. Additionally, one might expect the hybridization of the nitrogen atoms to be affected.

To put these qualitative arguments on a quantitative footing would ideally require optimization of the geometry of the molecule in the ICT state, but this poses practical problems. Although optimization at the TD-DFT level has recently become possible,<sup>47–49</sup> it has not yet been implemented in the GAUSSIAN suite of programs, while geometry optimization at the CASSCF level is prohibited by the size of the molecule. To assess whether the experimentally observed Stokes shift is nevertheless compatible with our ideas, we have performed a number of calculations that are inconclusive when considered separately but when taken together support our interpretation of the experimental observations.

The first remark to be made is that the geometry relaxation taking place in the dimethylamino groups by internal charge transfer should also occur upon removal of an electron from the 1 orbital by ionization. The associated  $1^2B$  ( $1^{-1}$ ) state (in  $C_2$  symmetry) may therefore serve as a model for the geometry changes of the dimethylamino groups upon excitation to the ICT state. Optimization at the UB3LYP/6-31G\* level shows that the ion adopts a conformation of  $C_{2v}$  symmetry—and thus becomes of  $2^2B_2$  ( $1^{-1}$ ) symmetry—with extended amino–ring bonds and dimethylamino groups which are perpendicular to the naphthalene plane (Table 2). Apparently, the reduced charge density in the lone pair orbitals permits a reduction of the steric interactions through a rotation of the two dimethylamino groups. The internal reorganization energy upon ionization is obtained from the difference between vertical (7.02 eV) and adiabatic ionization energies (6.35 eV) as 0.67 eV. In a simple model, in which the Stokes shift of the ICT state is only associated with the geometry relaxation of the dimethylamino groups and vibrational coordinates and frequencies remain the same in

ground and excited state, this would imply a Stokes shift of 1.34 eV, which is remarkably close to the experimental number.

The  $^1L_a$  state also has a partial charge-transfer character owing to the contributions from the dimethylamino lone pair orbitals to the HOMO. It might therefore undergo significant geometry relaxation as well. In view of this observation, it is interesting to see how the molecular geometry responds to ionization of an electron from the HOMO. Optimization of the molecular geometry in the associated  $1^2A$  ( $\pi_5^{-1}$ ) ionic state demonstrates that the molecule is indeed subject to considerable geometry changes (Table 2), but in just the opposite way as was observed for the  $1^2B$  ( $1^{-1}$ ) state: instead of an enhanced twisting, an untwisting motion occurs by which the dimethylamino lone pair orbitals become nearly parallel with the  $\pi$ -orbitals of the naphthalene moiety. Concurrently, the amino–ring bonds become shorter and the deviation from planarity of the naphthalene skeleton larger. Apparently, it is now the enlarged conjugation of the  $\pi$  electron system that is the dominant driving force for the geometry relaxation. For the  $1^2A$  ( $\pi_5^{-1}$ ) state vertical and adiabatic ionization energies of 6.81 and 6.03 eV, respectively, are calculated, implying that the internal reorganization energy for this state (0.78 eV) is even larger than for the  $1^2B$  ( $1^{-1}$ ) state.

The vertical and adiabatic ionization potentials that we calculate for the  $1^2A$  ( $\pi_5^{-1}$ ) and  $1^2B$  ( $1^{-1}$ ) states are in good agreement with the He(I) photoelectron spectrum of DMAN,<sup>50</sup> which shows two bands at 7.05 and 7.45 eV in this energy region. For the first band an adiabatic ionization energy of 6.45 eV has been reported, but the width of the bands precludes the determination of the adiabatic ionization energy for the second band. In agreement with the present results, the He(I) study concluded that for twisted dimethylamino groups the two bands are associated with the  $1^2A$  ( $\pi_5^{-1}$ ) and  $1^2B$  ( $1^{-1}$ ) states, respectively.

The second remark to be made is that in the excited states of the neutral molecule electron density is not removed but redistributed, and we therefore need to determine to what extent the geometry relaxations in the ionic states persist in the excited states of the neutral molecule. UB3LYP calculations of the  $^31\pi_6^*$  and  $^3\pi_5\pi_6^*$  electronic configurations—which are the dominant configurations in the description of the  $1^3B$  ( $T_2$ ) and  $1^3A$  ( $T_1$ ) states as shown by TD-DFT calculations on the triplet manifold—may serve to investigate this issue. Above, the importance of dynamic electron correlation has become clear, which is the principal reason we insist on the DFT quality of the calculation. However, a complete description of the two triplet states would obviously require that nondynamical electron correlation as well is taken into account. At this point, however, we are merely interested in the effect of the electron density redistribution and will continue to consider only the aforementioned configurations. Similar to the  $1^2B$  ( $1^{-1}$ ) state, we find that the geometry of lowest energy for the  $1^3B$  ( $T_2$ ) state has  $C_{2v}$  symmetry (and is thus more appropriately labeled as  $1^3B_1$ ) (Table 2) with geometrical parameters resembling those of the  $1^2B$  ( $1^{-1}$ ) state. The main differences are found in the bond lengths within the naphthalene skeleton that are changed reflecting the (anti)bonding properties of the  $\pi_6^*$  orbital. Comparison with the energy of this state at the  $S_0$  equilibrium geometry leads to an internal reorganization energy of 0.79 eV. This is slightly higher than found for the  $1^2B$  ( $1^{-1}$ ) state, as might have been anticipated from the decoupled nature of the two unpaired electrons at this geometry. Interestingly, we calculate for the dipole moment of the molecule at the equilibrium

geometry of the excited state a value of 7.7 D, which agrees nicely with the dipole moment of the emissive state inferred from our experiment.

Optimization of the molecular geometry for the  $1^3A$  state results in a  $C_2$  conformation of lowest energy that still has partly untwisted dimethylamino groups, albeit that less untwisting occurs than in the corresponding cationic state (Table 2). The nonplanarity of the naphthalene skeleton, on the other hand, is slightly increased. For this state a geometry relaxation energy of 0.41 eV is found, almost half of that in the  $1^2A$  ( $\pi_5^{-1}$ ) state. Since for this geometry the two unpaired electrons are far from decoupled, this result is not so surprising.

The calculations discussed above lead to a number of conclusions. First, the internal reorganization energies obtained are almost in quantitative agreement with the experimentally observed one, thereby supporting the conclusion that geometry relaxation is the dominant cause of the observed Stokes shift. Second, the calculations suggest that in the emissive state monitored by experiment the molecule adopts a conformation in which the dimethylamino groups are subject to significant twisting, even to such an extent that the dimethylamino lone pair orbitals are decoupled from the naphthalene  $\pi$ -system. This conclusion is corroborated by our transient absorption experiments, which show that upon excitation a naphthalene radical-anion-like species is formed. Third, owing to its partial charge-transfer character, the  $^1L_a$  state as well is subject to geometry relaxation involving the dimethylamino groups. However, the calculations indicate that the dimethylamino groups are now subject to an untwisting motion. Experimental support for this conclusion can be found in the high-resolution spectroscopic studies performed on (un)substituted 1-aminonaphthalenes in the gas phase.<sup>17,18</sup> For these molecules, which have the  $^1L_a$  state as the lowest excited singlet state (vide supra), it has been demonstrated that the amino group undergoes an untwisting motion upon excitation.

#### IV. Conclusions

The final picture that emerges from the theoretical calculations compares favorably with the experimental results obtained in the present studies. The vertical excitation energy for the lower two excited states nicely reproduces the gas-phase results and the maximum of the first absorption band in nonpolar solvents. Comparison of the observed molecular extinction coefficient of this band with the calculated oscillator strengths for the two quasi-degenerate  $1\pi^*$  and  $\pi\pi^*$  transitions shows that we are predominantly exciting the  $^1L_a$ -type state in our experiments. This state is not responsible for the observed emission as can be inferred from the radiative decay rate but merely acts as doorway to the electronically excited-state manifold, after which internal conversion populates the  $1\pi^*$  state. The intrinsic internal charge transfer character of this state, which is confirmed by the transient absorption spectra that carry the signature of the naphthalene radical anion, explains the relatively large dipole moment inferred from the solvent dependence of the emission. Compared to various 1-amino-substituted naphthalenes, the vertical excitation energy of the  $1\pi^*$  state appears to be considerably lowered, which is attributed to the steric strain and lone pair repulsion that accompanies the introduction of the second dimethylamino group in DMAN. Owing to a relief of the repulsive interaction between the nitrogen lone pair orbitals, the  $1\pi^*$  state is subject to considerable internal reorganization effects that are ultimately responsible for the large Stokes shift already observed in nonpolar solvents. The calculations and transient absorption experiments indicate that the geometry



relaxation predominantly involves an increased twisting of the dimethylamino groups. For the  $^1L_a$ -type state, a significant geometry relaxation is likewise predicted, albeit in the opposite direction: the dimethylamino groups now untwist, a motion by which conjugation is extended. These large-amplitude motions as well as the various energy relaxation pathways are subject of a forthcoming publication in which studies are reported using femtosecond transient absorption and fluorescence upconversion techniques.<sup>51</sup>

**Acknowledgment.** This work was supported by The Netherlands Organization for Scientific Research (NWO). A.S.-H. thanks Prof. L. Sobczyk and Prof. A. Koll (Faculty of Chemistry, Wrocław University) as well as Dr. I. Deperasińska (Institute of Physics of Polish Academy of Sciences, Warsaw) and Dr. A. Kapturkiewicz (Institute of Physical Chemistry of Polish Academy of Sciences-Warsaw) for helpful discussions. She is also grateful to the Royal Dutch Academy of Arts and Sciences (KNAW) and The Netherlands Organization for Scientific Research (NWO) for financial support to participate in the experimental work at the University of Amsterdam. We wish to thank Dr. F. Hulsbergen (Leiden University) and J. van Ramesdonk (University of Amsterdam) for experimental assistance, and Dr. A. M. Brouwer (University of Amsterdam) for illuminating discussions.

## References and Notes

- (1) Staab, H. A.; Saupe, T. *Angew. Chem., Int. Ed. Engl.* **1988**, *27*, 865.
- (2) Alder, R. W. *Chem. Rev.* **1989**, *89*, 1215.
- (3) Hibbert, F. J. *J. Chem. Soc., Perkin. Trans.* **1974**, *2*, 1862.
- (4) Lou, Yan K.; Saluja, P. P. S.; Kebarle, P.; Alder, R. W. *J. Am. Chem. Soc.* **1978**, *100*, 7328.
- (5) Llamas-Saiz, A. L.; Foces-Foces, C.; Elguero, J. *J. Mol. Struct.* **1994**, *328*, 297.
- (6) Hibbert, F.; Hunte, K. P. *J. Chem. Soc., Perkin Trans.* **1983**, *2*, 1895.
- (7) Boussif, O.; Lezoualch, F.; Zanta, M. A.; Mergny, M. D.; Scherman, D.; Demeneix, B.; Behr, J. P. *Proc. Natl. Acad. Sci.* **1995**, *92*, 7297.
- (8) Behr, J. P. *Chimia* **1997**, *51*, 34.
- (9) Perrin, C. L.; Ohta, B. K. *J. Am. Chem. Soc.* **2001**, *123*, 6520.
- (10) Einspar, H.; Robert, J. B.; Marsh, R. E.; Roberts, J. D. *Acta Crystallogr.* **1973**, *B29*, 1611.
- (11) Malinson, P. R.; Woźniak, K.; Smith, G. T.; McCormack, K. L. *J. Am. Chem. Soc.* **1997**, *119*, 11502.
- (12) Malinson, P. R.; Woźniak, K.; Wilson, C. C.; McCormack, K. L.; Yufit, D. S. *J. Am. Chem. Soc.* **1999**, *121*, 4640.
- (13) Howard, S. T. *J. Am. Chem. Soc.* **2000**, *122*, 8238.
- (14) Szemik-Hojniak, A.; Zwier, J. M.; Buma, W. J.; Bursi, R.; van der Waals, J. H. *J. Am. Chem. Soc.* **1998**, *120*, 4840.
- (15) Szemik-Hojniak, A.; Deperasińska, I.; Allonas, X.; Jacques, P. *J. Mol. Struct.* **2000**, *526*, 219.
- (16) Meech, S. R.; O'Connor, D. V.; Philips, D.; Lee, A. G. *J. Chem. Soc., Faraday Trans. 2* **1983**, *79*, 1563.
- (17) Berden, G.; Meerts, W. L.; Plusquellic, D. F.; Fujita, I.; Pratt, D. W. *J. Chem. Phys.* **1996**, *104*, 3935.
- (18) Lahmani, F.; Zehnacker-Rentien, A.; Coudert, L. H.; Zachariasse, K. A. *J. Phys. Chem. A* **2003**, *107*, 7364.
- (19) Zachariasse, K. A.; Grobys, M.; von der Haar, Th.; Hebecker, A.; Il'ichev, V.; Yu, V.; Jiang, Y. B.; Morawski, O.; Rückert, I.; Kühnle, W. *J. Photochem. Photobiol. A: Chem.* **1997**, *105*, 373.
- (20) Suzuki, K.; Tanabe, H.; Tobita, S.; Shizuka, H. *J. Phys. Chem. A* **1997**, *101*, 4496.
- (21) Rückert, I.; Demeter, A.; Norawski, O.; Kühnle, W.; Tauer, E.; Zachariasse, K. A. *J. Phys. Chem. A* **1999**, *103*, 1958.
- (22) Suzuki, K.; Demeter, A.; Kühnle, W.; Tauer, E.; Zachariasse, K. A.; Tobita, S.; Shizuka, H. *Phys. Chem. Chem. Phys.* **2000**, *2*, 981.
- (23) Szemik-Hojniak, A.; Rettig, A.; Deperasińska, I. *Chem. Phys. Lett.* **2001**, *343*, 404.
- (24) Eaton, D. F. *J. Photochem. Photobiol. B-Biol.* **1988**, *2*, 523.
- (25) Armarego, W. L. F.; Perrin, D. D. *Purification of Laboratory Chemicals*, 2nd ed.; Pergamon Press Ltd.: Oxford, England, 1980.
- (26) Van Dijk, S. I.; Wiering, P. G.; Groen, C. P.; Brouwer, A. M.; Verhoeven, J. W.; Schuddeboom, W.; Warman, J. M. *J. Chem. Soc., Faraday Trans.* **1996**, *91*, 2107.
- (27) Mataga, N.; Kaifu, Y.; Koizumi, M. *Bull. Chem. Soc. Jpn.* **1955**, *28*, 690.
- (28) Lippert, E. *Z. Elektrochem.* **1957**, *61*, 962.
- (29) Pozharsky, A. F.; Alexandrov, G. G.; Vistorobski, N. V. *Zh. Org. Khim.* **1991**, *27*, 1536.
- (30) Il'ichev, Y. V.; Kühnle, W.; Zachariasse, K. A. *Chem. Phys.* **1996**, *211*, 441.
- (31) Strickler, S. J.; Berg, R. A. *J. Chem. Phys.* **1962**, *37*, 814.
- (32) Bebelaar, D. *Chem. Phys.* **1974**, *3*, 205.
- (33) Brun, A. M.; Harriman, A.; Tsuboi, Y.; Okada, T.; Mataga, N. *J. Chem. Soc., Faraday Trans.* **1995**, *91*, 4047.
- (34) Shida, T. *Electronic Absorption Spectra of Radical Ions*; Elsevier: Amsterdam, 1988.
- (35) The absorption spectrum of the radical anion of 1,8-diaminonaphthalene is very similar to that of the radical anion of naphthalene, albeit that the bands are somewhat shifted and that it is less structured.
- (36) Sobolewski, A. L.; Sudholt, W.; Domcke, W. *J. Phys. Chem. A* **1998**, *102*, 2716.
- (37) Parusel, A. B. J.; Rettig, W.; Sudholt, W. *J. Phys. Chem. A* **2002**, *106*, 804.
- (38) Rappoport, D.; Furche, F. *J. Am. Chem. Soc.* **2004**, *126*, 1277.
- (39) Frisch, M. J.; Trucks, G. W.; Schlegel, H. B.; Scuseria, G. E.; Robb, M. A.; Cheeseman, J. R.; Zakrzewski, V. G.; Montgomery, J.; Stratmann, R. E.; Burant, J. C.; Dapprich, S.; Millam, J. M.; Daniels, A. D.; Kudin, K. N.; Strain, M. C.; Farkas, O.; Tomasi, J.; Barone, V.; Cossi, M.; Cammi, R.; Mennucci, B.; Pomelli, C.; Adamo, C.; Clifford, S.; Ochterski, J.; Petersson, G. A.; Ayala, P. Y.; Cui, Q.; Morokuma, K.; Malick, D. K.; Rabuck, A. D.; Raghavachari, K.; Foresman, J. B.; Cioslowski, J.; Ortiz, J. V.; Stefanov, B. B.; Liu, G.; Liashenko, A.; Piskorz, P.; Komaromi, I.; Gomperts, R.; Martin, R. L.; Fox, D. J.; Keith, T.; Al-Laham, M. A.; Peng, C. Y.; Nanayakkara, A.; Gonzalez, C.; Challacombe, M.; Gill, P. M. W.; Johnson, B.; Chen, W.; Wong, M. W.; Andres, J. L.; Gonzalez, C.; Head-Gordon, M.; Replogle, E. S.; Pople, J. A. *Gaussian 98, Revision A.5*. Gaussian, Inc.: Pittsburgh, PA, 1998.
- (40) Frisch, M. J.; Pople, J. A.; Binkley, J. S. *J. Chem. Phys.* **1984**, *80*, 3265.
- (41) Foresman, J. B.; Head-Gordon, M.; Pople, J. A.; Frisch, M. J. *J. Chem. Phys.* **1992**, *96*, 135.
- (42) Becke, A. M. *J. Chem. Phys.* **1993**, *98*, 5648.
- (43) Calculation of the harmonic force field at the optimized  $C_2$  geometry shows that this geometry is actually a minimum on the potential energy surface. We can thus conclude that the conformation of lowest energy in the ground state is at the B3LYP/6-31G\* level predicted to be of  $C_2$  symmetry.
- (44) Kasha, M.; Rawls, H. R. *Photochem. Photobiol.* **1968**, *7*, 561.
- (45) In the past, calculations on the excited states of 1-(dimethylamino)naphthalene have been performed at the CIS/STO-3G and CIS/3-31G level.<sup>20</sup>
- (46) The B3LYP/6-31G\* structure was found to be nearly identical with the one previously reported employing the 6-31G\*\* basis set.<sup>18</sup>
- (47) Van Caillie, C.; Amos, R. D. *Chem. Phys. Lett.* **2000**, *317*, 159.
- (48) Furche, F.; Ahlrichs, R. *J. Chem. Phys.* **2002**, *117*, 7433.
- (49) Hutter, J. *J. Chem. Phys.* **2003**, *118*, 3928.
- (50) Maier, J. P. *Helv. Chim. Acta* **1974**, *57*, 994.
- (51) Balkowski, G.; Szemik-Hojniak, A.; van Stokkum, I. H. M.; Zhang, H.; Buma, W. J. To be published.